

Persistence of Molecular Orientation in Adsorbed Ethylene–Vinyl Acetate Copolymer Nanofilm Studied by Fourier Transform Infrared Reflectance Spectroscopy

Maurice Brogly,* Sophie Bistac, and Jacques Schultz

Université de Haute-Alsace, CNRS-Institut de Chimie des Surfaces et des Interfaces,
15 rue Jean Starcky, B.P. 2488, F-68057 Mulhouse Cedex, France

Received September 23, 1997; Revised Manuscript Received March 9, 1998

ABSTRACT: FTIR reflectance experiments have been performed on thin ethylene–vinyl acetate (EVA) copolymer layers deposited on aluminum mirrors in order to determine the orientation of polymer functional groups at the interface. This was accomplished by using various reflection angles under p-polarization states of the incident IR wave. Film thickness is estimated by ellipsometric experiments. Kramers–Kronig analysis is first applied to the external infrared reflection spectrum from a single copolymer surface measured near the normal incidence angle. Absorption spectra, $k(\nu)$, are then deduced and used to calculate specular reflectance intensities of the functional groups of interest, as a function of reflection angle, polarization state, and film thickness. The calculated values are compared to the experimental ones. An original layer model was developed and allows us to determine the persistence length of the molecular orientation of EVA carbonyl groups at the interface. This approach is based on the fact that molecular orientation persists only over a given distance from the geometrical interface. This distance is called the “persistence length of molecular orientation”. We then suppose that the nanofilm adsorbed is stratified and consists of an oriented layer (in the near interface region) plus an isotropic one. It seems that only carbonyl groups involved in specific electron donor–electron acceptor interactions at the interface are subjected to specific orientation.

Introduction

The formation, structure, and properties of organic macromolecular thin films are subjects of current interest. Some important questions on their structure such as molecular orientation and conformational changes due to macromolecular adsorption should be asked in order to solve problems related to adhesion. Central to a comprehensive understanding of molecular aspects of adhesion is the determination of the molecular structure (specific interactions, changes in conformations, and molecular orientation) at the polymer/metal interface. While a number of surface analysis tools are available, in actual fact, only a few are applicable to the analysis of the subtle features of the chemical structures of complicated macromolecular thin films adsorbed onto metallic substrates. Surface techniques using ions or electrons as probes¹ should be excluded because of damage caused to organic molecules. We have thus selected FTIR reflectance spectroscopy^{2–4} that uses photon probes for the determination of the molecular structure of poly(ethylene-*co*-vinyl acetate) adsorbed onto aluminum mirrors. The orientation of polymer functional groups at the interface was studied by performing experiments at various reflection angles under p-polarization states of the incident IR wave. Film thickness is estimated by ellipsometry. Specular reflectance intensities of the functional groups concerned, as a function of reflection angle, polarization state, and film thickness were calculated and compared to the observed ones. An original layer model was developed and allows us to determine the molecular orientation of EVA carbonyl groups at the interface. Although the determination of orientation in molecular assemblies is

the subject to numerous studies,^{5–7} not one is devoted to the determination of the orientation of the adsorbed copolymer. Moreover, all studies consider that orientation remains in all the adsorbed film. This is not realistic. In fact, we consider that in the near-interface region functional groups may be oriented. This orientation remains on a certain depth we propose to call the “orientation persistence length”. Above, the system is assumed to be isotropic, and no orientation persists. It seems that only carbonyl groups involved in specific electron donor–electron acceptor interactions at the interface are subject to this specific orientation.

Theoretical Background

Band Intensity Calculations. The theory that relates the macroscopic variables of the experiment to the propagating incident and reflected electric fields, adapted for reflectance spectroscopy in a multilayered medium, have been described in the literature.⁸ The mathematical treatment of a multiphase system is done by Heavens matrix analysis,⁹ where each phase is characterized by a matrix that relates the electric and magnetic fields at the two boundaries. An original Kramers–Kronig analysis is first used to determine the complex refractive index of the poly(ethylene-*co*-vinyl acetate) polymer, on the basis of external reflection experiments near the normal angle of reflection (angles ranging from 5 to 8°). Kramers–Kronig analysis for a reflection spectrum from a single interface has often been used to obtain a complex refractive index, because the real part of the complex reflectivity is directly measured as the reflectivity. The phase shift after reflection can be calculated according to the works of Dignam,¹⁰ Bardwell and Dignam,¹¹ and Dignam and Mamiche-Afara.¹² In this last paper, the author found very good correlation for polymers that have an absorp-

* Corresponding author. Tel: (0) 3 89 60 87 68. Fax: (0) 3 89 60 87 99. E-mail: M.Brogly@univ-mulhouse.fr.

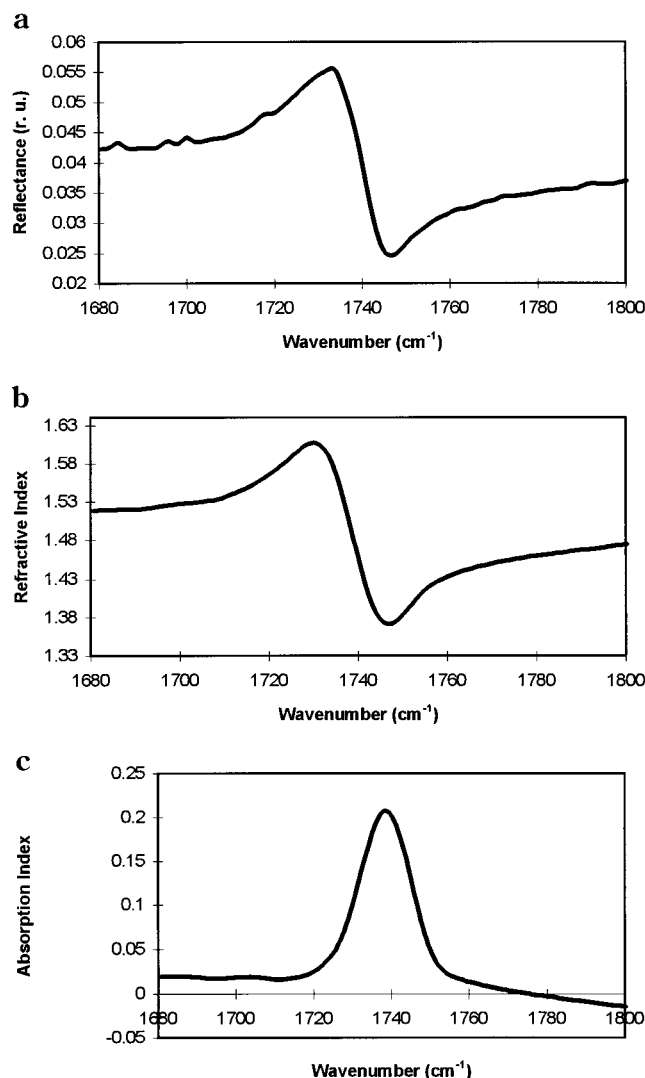


Figure 1. (a) Experimental EVA copolymer reflectance spectrum at 5° reflection angle in the C=O 1680–1800 cm⁻¹ absorption region. (b) Frequency dependence of the real part, $n(\nu)$, of the EVA complex refractive index. (c) Frequency dependence of the imaginary part, $k(\nu)$, of the EVA complex refractive index.

tion index k lower than 0.9. The phase calculation was also in agreement with a calculation developed by Ishida^{13,14} and co-workers. All these algorithms give accurate results for transition moments that exhibit a rather strong absorption coefficient k . This is the case of the C=O band of the EVA. In a well-known paper, Urban¹⁵ propose another correction algorithm based on double Kramers–Kronig transformation applicable for weak and strong bands. The procedure is to calculate the phase shift by a classical KK transformation. Injection of the phase in Fresnel equations⁸ gives \mathbf{k} . This later gives \mathbf{n} after a second KK transformation. Results are quite identical with both methods for the C=O band.

The frequency dependence of the real, \mathbf{n} , and imaginary parts, \mathbf{k} , of the complex refractive index, $\hat{n}(\nu) = n(\nu) - ik(\nu)$ of an optically thick sample are shown in Figure 1b,c, respectively.

Reflection–absorption experiments are generally conducted to obtain properties such as glass transition temperature¹⁶ or molecular orientation¹⁷ of thin films adsorbed on reflecting plane substrates such as metals. It is well-known that under p-polarization (i.e., parallel to the incident wave plane) a standing wave is generated

at the interface of reflection that magnifies the IR signal.¹⁸ This effect increases as the reflection angle does and, at grazing angles, nanolayers can be studied. Concerning specular reflectance under p-polarization, the following equations are used to simulate the optical behavior of a multiphase system. Fresnel complex reflectivity between two mediums i and j , of indices $\hat{n}_i(\nu) = n_i(\nu) - ik_i(\nu)$ and $\hat{n}_j(\nu) = n_j(\nu) - ik_j(\nu)$, is expressed as follows:

$$\hat{r}_{ij}^P = \{ (n_j^2(\nu) - k_j^2(\nu) - i2n_j(\nu)k_j(\nu))\hat{n}_i(\nu)\cos(\theta_i) - (n_i^2(\nu) - k_i^2(\nu) - i2n_i(\nu)k_i(\nu))\hat{n}_j(\nu)\cos(\theta_j) \} / \{ (n_j^2(\nu) - k_j^2(\nu) - i2n_j(\nu)k_j(\nu))\hat{n}_i(\nu)\cos(\theta_i) + (n_i^2(\nu) - k_i^2(\nu) - i2n_i(\nu)k_i(\nu))\hat{n}_j(\nu)\cos(\theta_j) \} \quad (1)$$

For a three-phase system where the ambient medium is air, the EVA polymer is the second medium ($\hat{n}_2(\nu)$), and the substrate is the third medium ($\hat{n}_3(\nu)$), the complex reflectivity and power reflectivity are respectively

$$\hat{r}_{123}^P(\nu) = \frac{\hat{r}_{12}^P(\nu) + \hat{r}_{23}^P(\nu) \exp \frac{-i4\pi\hat{n}_2(\nu)d\cos(\theta_2)}{\lambda}}{1 + \hat{r}_{12}^P(\nu)\hat{r}_{23}^P(\nu) \exp \frac{-i4\pi\hat{n}_2(\nu)d\cos(\theta_2)}{\lambda}} \quad \text{and} \quad R_{123}^P(\nu) = \hat{r}_{123}^P(\nu)\hat{r}_{123}^{*P}(\nu) \quad (2)$$

This mathematical algorithm is used to simulate reflectance experiments and is capable of handling any number of phases and gives exact solutions within the limits of classical electromagnetic theory and linear optics.

Molecular Orientations Calculations. The orientation of adsorbate molecular groups that have infrared active modes can be calculated from reflection spectra because of the anisotropy of the electric field generated at the polymer/metal interface. It follows that, for the grazing angle of reflection of a p-polarized infrared beam off most metals, the effective contribution to the electric field is normal to the surface ($\mathbf{E}'' \approx \mathbf{E}_z''$ and the z -direction is normal to the surface). Since the intensity of a given mode is proportional to the square of the scalar product of the electric field \mathbf{E} and the transition moment \mathbf{M} (or dipole moment derivative) with respect to the normal coordinate, it follows that the mode intensity of a functional group i will vary with its orientation at the surface (with respect to the z -direction normal to the surface) according to

$$I_i \propto |\mathbf{M}_{i,z} \cdot \mathbf{E}_z''|^2 = |M_i \cos(\varphi) \mathbf{z} \cdot \mathbf{E}_z''|^2 = M_i^2 E_z''^2 \cos^2(\varphi) \quad (3)$$

where φ is defined as the angle between the transition moment and the surface plane.

When the adsorbate overlayer is anisotropic (i.e., subjected to specific molecular orientation) but otherwise identical to the bulk structure, let us first consider the case of a thin layer where all the N transition moments of a functional group i are oriented normally to the surface (i.e., in the z -direction). The measured intensity is then proportional to

$$I_i^{z\text{-orientation}} \propto \sum_{j=1}^N |\mathbf{M}_{j,(i,z)} \cdot \mathbf{E}_z''|^2 = \sum_{j=1}^N |M_{j,(i)} \mathbf{z} \cdot \mathbf{E}_z''|^2 = M_i^2 E_z''^2 \quad (4)$$

On the contrary, if the N transition moments of a

functional group i are randomly distributed in this layer (i.e., isotropic), then the intensity is proportional to

$$I_i^{\text{isotropic}} \propto \sum_{j=1}^N |\mathbf{M}_{j,i,z} \cdot \mathbf{E}_z''|^2 = \sum_{j=1}^N |M_{j,i} \cos(\varphi_j) \mathbf{z} \cdot \mathbf{E}_z''|^2 = M_i^2 E_z''^2 \langle \cos^2(\varphi) \rangle \quad (5)$$

The average value of the orientation angle can easily be deduced and is equal to

$$\langle \cos^2(\varphi) \rangle = \frac{I_i^{\text{polymerlayer}}}{3I_i^{\text{isotropic}}} \quad (6)$$

where $I_i^{\text{polymerlayer}}$ represents the intensity experimentally measured on a thin polymer layer/metal system and $I_i^{\text{isotropic}}$ represents the calculated value of the intensity reflected by an isotropic and homogeneous layer (of identical thickness) of the considered polymer. Of course, smaller differences may arise because of the correction required for the changes in the surface field due to an anisotropic polymer refractive index, $\hat{n}_2(\nu)$ (i.e., $\hat{n}_2(\nu)$ should be formulated as a tensor rather than a scalar). However, these changes are sufficiently small that they can be neglected. Other errors can arise due to the effects of surface roughness.¹⁹ The roughness scale of our samples is on the size $\sim 100 \times 100$ Å rounded low hills, as determined from atomic force microscopy (AFM). At this scale, the major point to note is that the measured orientation of the adsorbate molecules determined by IR is relative to the normal tangent of the surface curvature (the tangential electric field will be close to zero by simple electrostatic arguments for good conductors). Other effects have to do with the absolute values of band intensities of the local electric field in the vicinity of the oscillators. As discussed by Kotler,²⁰ these effects are not expected to be significantly different from the ideal surface values.

Molecular Orientation Persistence Length. Assuming that molecular orientation does not persist in the whole film thickness, we propose to determine the molecular orientation persistence length, O_{PL} . This determination is based on a two-layer model. We consider that the adsorbed film of thickness T is stratified and consists of an orientated layer, L_1 , of thickness $T_1 = O_{\text{PL}}$ plus an isotropic layer, L_2 , of thickness T_2 , and $T = T_1 + T_2$. Of course, because of the depth-dependent property of the mean square electric field, the range of thickness validity of the hereafter proposed model is limited to 1–20 nm. To a first approximation, the complex refractive index of the polymer is identical in both layers. To assess O_{PL} , IRAS measurements must be conducted at various angles of reflection. For p-polarization and for angles that deviate from grazing values, the electric field has two components, \mathbf{E}_x'' and \mathbf{E}_z'' . Surface reflectance is then proportional to the mean square electric field components. Exact values of the electric field intensities in stratified medium are discussed by Hansen.²¹ The mode intensity of a functional group i , will vary with its orientation, φ , at the surface and with the angle of reflection of the plane electric field, θ . The electric field vector has two components, \mathbf{E}_x'' and \mathbf{E}_z'' and the transition moment can also be separated into two contributions. The development of the scalar product of the electric field and transition moment vector is expressed as follows:

$$I_i^{\text{oriented}} \propto |\mathbf{M}_i \cdot \mathbf{E}''|^2 = (\mathbf{M}_{i,x} + \mathbf{M}_{i,z}) \cdot (\mathbf{E}_x'' + \mathbf{E}_z'')^2 \quad (7)$$

where I_i^{oriented} is the band intensity of the oriented layer. We define the transition moment and electric field vectors as

$$\mathbf{M}_i = M_i \langle \sin(\varphi) \rangle \mathbf{x} + M_i \langle \cos(\varphi) \rangle \mathbf{z} \quad \text{and} \\ \mathbf{E}'' = E' \cos(\varphi) \mathbf{x} + E' \sin(\varphi) \mathbf{z} \quad (8)$$

Replacing eq 11 in eq 10, assuming the scalar product $xz = 0$, and using trigonometric rules in the case of sine and cosine cross products lead to

$$I_i^{\text{oriented}} \propto M_i^2 E'^2 |\sin(\theta + \langle \varphi \rangle)|^2 \quad (9)$$

Then, assuming that polymer optical constants remain unchanged in both oriented and isotropic layers, the intensity of the bilayer is the sum of the intensities of both oriented and isotropic layers. For an isotropic layer, the measured intensity is reduced to

$$I_i^{\text{isotropic}} \propto M_i^2 E'^2 \left| \sqrt{\frac{2}{3}} \cos(\theta) + \sqrt{\frac{1}{3}} \sin(\theta) \right|^2 \quad (10)$$

In the case of a stratified medium of thickness T , the intensity is expressed as

$$\frac{I_i^{\text{stratified}}}{I_i^{\text{isotropic}}} = \frac{T_2}{T} + \frac{O_{\text{PL}}}{T} \left| 3 \frac{\sin^2(\theta + \langle \varphi \rangle)}{|\sqrt{2} \cos(\theta) + \sin(\theta)|^2} \right| \quad (11)$$

If T is determined by ellipsometry, then only two unknown values, O_{PL} and $\langle \varphi \rangle$, persist in the system. Minimization algorithms, for the N reflection angles, θ_i , give the following implicit equation in $\langle \varphi \rangle$, which can easily be resolved:

$$\sum_{i=1}^N \left\{ 1 - \frac{I_i^{\text{stratified}}}{I_i^{\text{isotropic}}} - \frac{\sum_{j=1}^N \left(1 - \frac{I_j^{\text{stratified}}}{I_j^{\text{isotropic}}} \right) \left(\frac{3 \sin^2(\theta_i + \langle \varphi \rangle)}{(\sqrt{2} \cos(\theta_i) + \sin(\theta_i))^2} \right)}{\sum_{j=1}^N \left(\frac{3 \sin^2(\theta_j + \langle \varphi \rangle)}{(\sqrt{2} \cos(\theta_j) + \sin(\theta_j))^2} \right)^2} \right\} \times \frac{\sin(2\theta_i + 2\langle \varphi \rangle)}{(\sqrt{2} \cos(\theta_i) + \sin(\theta_i))^2} = 0 \quad (12)$$

Experimental Section

Sample Preparation. The sample studied in this work is an ethylene-vinyl acetate (EVA) copolymer having a molar vinyl acetate content of 18.9% mol/mol. This EVA exhibits a glass transition at 239 K. The vinyl acetate content is high enough to prevent crystallization of ethylene comonomers. The weight average molar mass and polydispersity index are respectively equal to 45 000 g/mol and 2.9. According to ¹³C NMR results, the branching content is 0.45%. Transition and phase morphology were fully described elsewhere.²² EVA was spin-coated onto a flat and polished aluminum mirror, from an EVA solution in chromatographic grade chloroform. Samples were then annealed for 1 h at 80 °C, to relax adsorbed macromolecular chains and remove solvent. The roughness of polished aluminum plates

was estimated to be less than 2 nm by atomic force microscopy (AFM).

The nanofilm thickness was estimated by using an ES4M spectroscopic ellipsometer by Sopra. The value obtained is equal to 120 Å.

IR Reflectance Measurements. Reflection FTIR spectra were measured on a Bruker IFS 66 FTIR spectrometer equipped with a liquid nitrogen cooled MCT detector. A total of 500 averaged scans of 2 cm^{-1} resolution gave experimental spectra, with accurate signal-to-noise ratio. The p-polarized reflection spectra were obtained by placing two wire-grid polarizers at the entrance and exit of the reflection apparatus. The reference spectrum was obtained with a polished aluminum mirror. Spectra were recorded at angles of reflection ranging from 20 to 85° . A near normal reflection (5° angle of reflection) specular reflection experiment allowed the determination of optical constants of EVA. Spectra analyses were done on OPUS software. IR band intensity simulation and molecular orientation persistence length were calculated using programs developed with MATHEMATICA software.

Results

Determination of Optical Constants. The EVA copolymer is characterized by its acetate group, especially the carbonyl (C=O) functionality, which exhibits strong absorption in the infrared. All the study will focus on the particular behavior of this functional group in the near interface region. The IR absorption intensity of the C=O group results from the combination of the dispersion of the refractive index and the strong absorption index at 1738 cm^{-1} , in the case of the stretching vibration mode. In a near normal reflection angle reflectance experiment the incident light beam is reflected only at the surface of the sample sheet in the region of strong absorption. Experimental reflection data were analyzed by performing double Kramers–Kronig transformation.¹⁵ The reflectance at normal reflection was evaluated by scaling²³ the observed reflectance measured at a 5° angle of reflection under p-polarization (see eqs 1 and 2):

$$R_p(0^\circ) = C_p R_p(5^\circ) \quad (13)$$

where $R_p(5^\circ)$ is the reflectance at an angle of reflection of 5° , for the incident radiation polarized parallel to the plane of reflection. The value of the scaling constant C_p is calculated to be 1.034 for EVA. Using double Kramers–Kronig transformation, the complex refractive index of an optically thick sample is determined. Figure 1a shows specular reflectance (5° reflection angle) spectra of EVA in the $1680\text{--}1800\text{ cm}^{-1}$ absorption region of the C=O group. Parts b and c of Figure 1 show the frequency dependence of the real ($n(\nu)$) and imaginary part ($k(\nu)$) of the complex refractive index of EVA. Values taken for optical constant at 1738 cm^{-1} are $\hat{n}_2 = 1.47 - i0.22$ for EVA and $\hat{n}_z = 3.7 - i94$ for the aluminum mirror. The complex refractive index of the aluminum mirror does not depend on frequency in the $1680\text{--}1800\text{ cm}^{-1}$ region.

Polarized Reflectance Spectra Analysis. Reflectance measurements were performed under reflection angles ranging from 20 to 85° , under p-polarization. Figure 2 represents the power reflectivity of a 120 Å EVA nanofilm adsorbed onto a smooth aluminum mirror for different angles of reflection, in the $1710\text{--}1770\text{ cm}^{-1}$

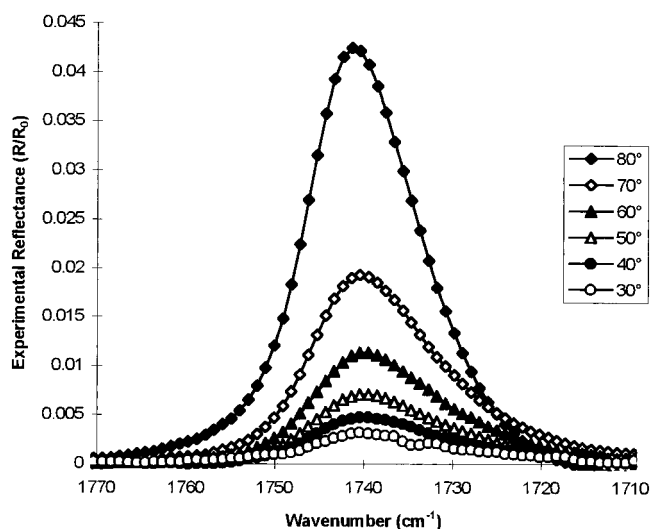


Figure 2. Experimental power reflectivity versus the angle of reflection of a 12 nm EVA nanofilm adsorbed onto an aluminum mirror.

absorption zone. Of course, the reflectivity decreases as the angle of reflection does, as predicted from the classical electromagnetic theory. To compare experimental reflectivity to simulated reflectivity, two important points must be discussed. First, it is well-known that reflectance spectra clearly show large changes in both peak position and shape compared to transmission spectra. These differences reflect spectroscopic artifacts²⁴ and not simply structural differences magnified by the nonequivalent thickness analyzed from one experiment (reflectance) to the other (transmission). Second, we have recently demonstrated²⁵ that the adsorption of EVA onto an aluminum mirror leads to the development of specific interactions at the interface. Indeed, electron acceptor–electron donor interactions (i.e., acid–base interactions in the Lewis sense²⁶) are favored between the C=O of the acetate group and superficial aluminol (Al–OH). C=O groups act as a Lewis base. A molecular orbital overlap exists between the LUMO and HOMO of both functional entities. This overlap strongly affects the C=O stretching frequency, leading to a splitting of the C=O absorption band in two contributions. A free one, which remains unchanged, and an acid–base one, which corresponds to vibrators involved in acid–base interactions at the interface. The magnitude of the frequency shift is directly related to the enthalpy of adduct formation.²⁷ Absorption bands in Figure 2 have two components as well. Before performing spectral decomposition of these bands, one should determine the spectral shape of the free C=O band in the case of reflectance experiments. In that way, eqs 1 and 2 allow us to simulate the band position and profile of an isotropic EVA layer onto aluminum, in the $1710\text{--}1770\text{ cm}^{-1}$ region. Complex refractive indices previously determined are used for calculation. Figure 3 shows the experimental profiles of a C=O band, as a function of reflection angle. Calculated profiles, in the free isotropic state, as represented in Figure 2, are then used to perform spectral deconvolution of the experimental band, as shown in Figure 4. Values of band intensities of free and acid–base bonded C=O bands as a function of the angle of reflection are gathered in Table 1. In the present case, the free component is located at 1742 cm^{-1} , whereas the acid–base one vibrates at 1735 cm^{-1} .

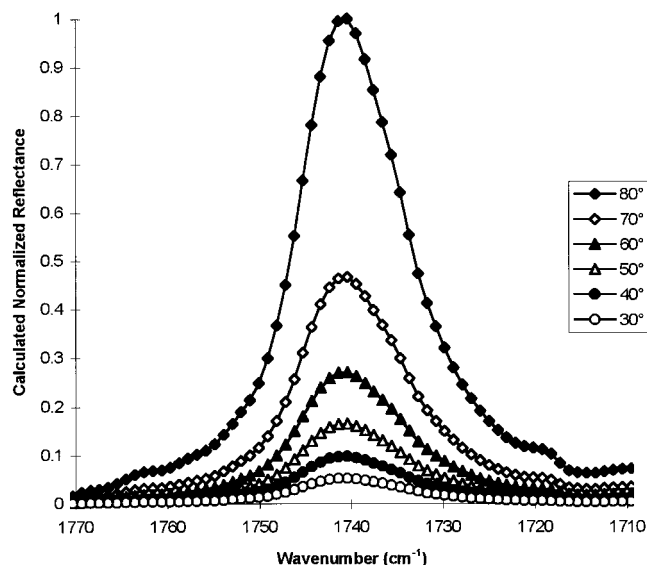


Figure 3. Calculated power reflectivity versus angle of reflection of an EVA nanofilm adsorbed onto an aluminum mirror.

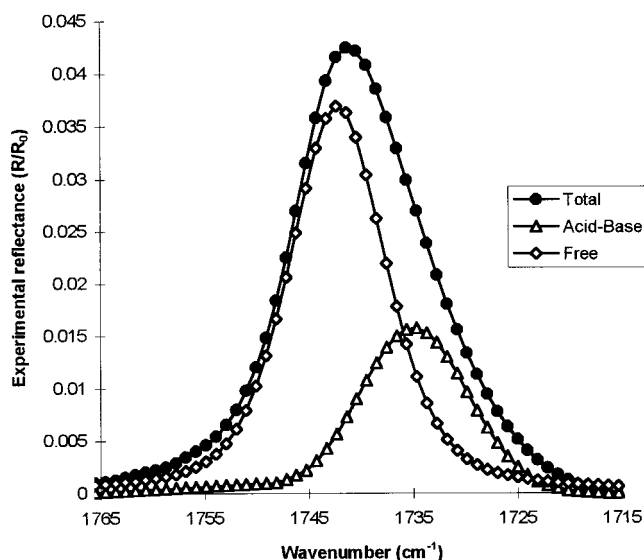


Figure 4. Free, acid-base bonded and total components of the C=O absorption band of a 12 nm EVA nanofilm onto an aluminum mirror ($\theta = 80^\circ$).

Band intensity simulations and molecular orientation persistence length. Equations (1) and (2) are used to calculate the power reflectivity at 1738 cm^{-1} of a three-phase system where medium 1 is air ($\hat{n}_1 = 1$), medium 2 is the EVA polymer ($\hat{n}_2 = 1.47 - i0.22$), and medium 3 is the aluminum mirror ($\hat{n}_3 = 3.7 - i94$). In fact, we calculate the following value:

$$-\log_{10}\left[1 - \frac{R^{\text{calculated}}}{R_0}\right] \quad (14)$$

where $R^{\text{calculated}}$ is the reflectivity of the three-phase system (air + polymer + aluminum mirror) and R_0 is the reflectivity of the aluminum mirror. Such calculations with isotropic bulk optical constants consider that the polymer is not submitted to preferential orientation in the adsorbed state; i.e., macromolecular chains remain in the isotropic state. We have reported in Figure 5 the difference between the experimental and

Table 1. Experimental Band Reflectivities vs Angle of Reflection: Free, Acid-Base, and Total Components

θ (deg)	$-\log_{10}[1 - (R_{\text{C=O}}^{\text{free}}/R_0)]$	$-\log_{10}[1 - (R_{\text{C=O}}^{\text{acid-base}}/R_0)]$	$-\log_{10}[1 - (R_{\text{C=O}}^{\text{total}}/R_0)]$
30	0.95×10^{-3}	0.27×10^{-3}	1.18×10^{-3}
40	1.68×10^{-3}	0.48×10^{-3}	1.97×10^{-3}
50	2.71×10^{-3}	0.79×10^{-3}	3.08×10^{-3}
60	4.49×10^{-3}	1.35×10^{-3}	4.94×10^{-3}
70	7.67×10^{-3}	2.45×10^{-3}	8.47×10^{-3}
80	16.33×10^{-3}	6.56×10^{-3}	18.68×10^{-3}

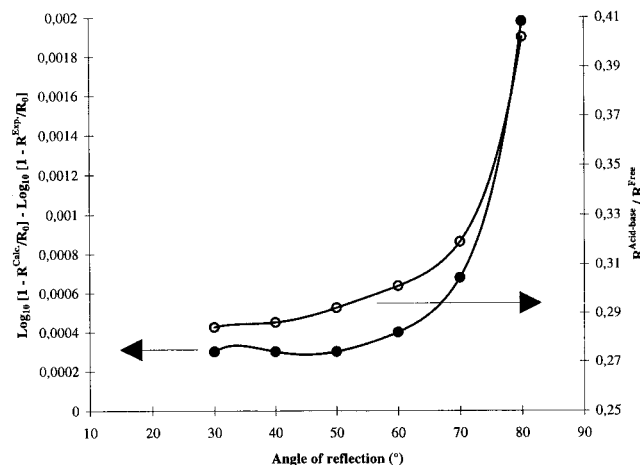


Figure 5. Differences between calculated and experimental power reflectivity of a 12 nm/aluminum mirror system vs the angle of reflection and the acid-base and free reflectivity ratio vs angle of reflection.

Table 2. Comparison between Calculated (Isotropic State) and Experimental Free Band Intensities and vs Angle of Reflection

θ (deg)	$-\log_{10}[1 - (R_{\text{C=O}}^{\text{free}}/R_0)]$	$-\log_{10}[1 - (R_{\text{C=O}}^{\text{calculated}}/R_0)]$
30	0.95×10^{-3}	0.88×10^{-3}
40	1.68×10^{-3}	1.64×10^{-3}
50	2.71×10^{-3}	2.76×10^{-3}
60	4.49×10^{-3}	4.54×10^{-3}
70	7.67×10^{-3}	7.79×10^{-3}
80	16.33×10^{-3}	16.70×10^{-3}

calculated reflectance of the 120 \AA EVA/aluminum system as a function of the IR beam angle of reflection. Important differences are observed at high angles of reflection. These differences may be due either to preferential molecular orientation in the adsorbed nanofilms or to systematic errors in the calculation routine. This latter point can easily be clarified by performing well-conducted experiments. Therefore, we have measured, on one hand, the power reflectivity of an EVA nanofilm adsorbed on a gold mirror and, on the other hand, we have the predicted power reflectivity. Results are consistent and the uncertainty interval does not exceed 0.4%. As a consequence, a full and correct interpretation of the differences in Figure 5 requires considering both orientation and bonding differences between isotropic bulk EVA and EVA macromolecular chains adsorbed on the aluminum mirror. Of course, both effects are linked. In other words, can interfacial acid-base force field act as a driving force to orient the interacting C=O groups at the interface and, if so, what is the molecular orientation persistence length within the adsorbed nanofilm?

Experimental (see Table 1) and calculated (see Table 2) power reflectivities are replaced in eq 11, and the implicit eq 12 is solved. Unicity of the solution is first verified. The following values for the molecular orienta-

tion persistence length O_{PL}^* , and average orientation angle relative to the surface plane $\langle\varphi\rangle^*$, are found:

$$O_{PL}^* = 29 \times 10^{-10} \text{ m} \quad \text{and} \quad \langle\varphi\rangle^* = 74^\circ \quad (15)$$

Discussion

According to the present IR experiments it seems that EVA macromolecular chains are preferentially oriented only in the vicinity of the interface. Moreover, we have previously evidenced that acid–base interactions are developed at the EVA/aluminum oxide interface. Different points should be discussed. The first point concerns the physical meaning of O_{PL}^* and $\langle\varphi\rangle^*$ values we have obtained. A molecular orientation persistence length value of 2.9 nm is comparable to the surface roughness magnitude, i.e., 2 nm of the aluminum substrate as determined by AFM. This tends to prove that only C=O groups of the first “monolayer” are subject to molecular orientation. One has to conclude that if O_{PL}^* reflects surface roughness, then only the C=O groups stuck at the surface are oriented. This supports the hypothesis that orbital overlapping between aluminum surface hydroxyls and EVA C=O basic groups promote the orientation of these latter. Such driving force action has been recently evidenced in the case of the adsorption of poly(methyl methacrylate) on an aluminum mirror.²⁸ If we assume that acid–base interactions promote adsorption and thus chain flattening, then the angle of 74° for the C=O sticky groups are with, on one hand, the minimum conformational energy of EVA, i.e., a 180° C–O–C=O dihedral angle and a 60° value of the CH₃–C–O–C dihedral angle of the acetate group and main chain axis, and on the other hand, the 126.19° angle value between the C=O group and C–O–C link. Indeed, such a conformation leads to an angle of 9.91° between the C=O group and the main chain axis, i.e., a value close to 80.09° between the surface plane and the C=O groups in the case of flat adsorption. Such a transition moment analysis²⁹ can be useful to understand experimental results.

A second point arises from the comparison between the experimental intensities of the “free” C=O stretching band and calculated values for an isotropic EVA layer of thickness $T - O_{PL}^*$ adsorbed on an aluminum mirror. These respective values are gathered in Table 2. A good agreement between experimental and calculated values is observed. This confirms that the reflectance IR signal of the “free” C=O stretching band is mainly due to isotropic C=O groups, i.e., not oriented and not involved in interfacial acid–base interactions. Moreover, the reflectivity ratio between acid–base and free components of the C=O absorption groups are strongly dependent on the angle of reflection. As shown in Figure 5, this ratio increases rapidly for high angles of reflection, proving that C=O groups involved in acid–base mechanisms are subject to preferential orientation. However, these results do not give information on the fraction of C=O groups of one chain that can be oriented. In other words, we are not able to discriminate between two possible schemes: the first one that considers that only loops or head and tail parts of the chain are stuck to the surface; and the second one that considers that acid–base driving forces can promote both chain flattening and functional group orientation.

A third point that would verify our conclusions about the tilt angle is to adsorb a 20 Å thick film and show it is completely oriented. We have the sensitivity and

know all the parameters for both oriented and isotropic films. We have done some experiments to obtain such a thin layer by spin-coating a highly diluted solution, 10^{−3} to 10^{−5} M. The problem is that the adsorption of EVA is not homogeneous at the molecular scale. Both atomic force microscopy (AFM) and wettability measurements have clearly demonstrated that the coverage is heterogeneous, that means an island of isolated chains plus uncovered domains. This effect is probably due to the fact that the radius of gyration of our chains is much greater than 20 Å, as determined by molecular dynamics calculations. Nevertheless, we have recently studied²⁸ the adsorption of nanofilms of stereoregular poly(methyl methacrylate). Depending on the tacticity, we have unambiguously evidenced that homogeneous films of 40–20 Å are realizable. In the case of pure isotactic poly(methyl methacrylate) we have observed chain flattening during adsorption. In the case of syndiotactic poly(methyl methacrylate) we have also measured an orientation of the skeletal backbone of the chains rather normal to the surface plane and with a persistence length in the 40 Å thickness. These results would constitute an original paper, which will soon be submitted for publication.

Conclusion

We have demonstrated in this study that accurate orientation information about EVA copolymer nanofilms on an aluminum mirror can be extracted from external reflection IR spectroscopy. Not only are average molecular orientations of the C=O groups of the adsorbed copolymer macromolecular chains determined, but also the persistence length within the film thickness is determined. This was possible thanks to the use of an original theoretical approach based on measurements at various angles of reflection, under p-polarization. The results presented here support the hypothesis that C=O groups involved in interfacial acid–base interactions are tilted by an average of 16° toward the normal surface. This orientation persists over about 29 Å within the film. Cooperative effects must exist between interfacial orbital overlapping, i.e., basic C=O groups and acid O–H aluminum oxide groups and molecular orientation. Further experiments should be done on EVA copolymers having VA content ranging from 40 to 70% w/w in order to highlight conformational effects on molecular orientation and associated persistence length. Molecular modeling predictions are also under calculation in order to correlate EVA φ – ψ map analysis with preferential adsorption.

References and Notes

- (1) Debe, M. K. *Prog. Surf. Sci.* **1987**, *24*, 1–4, 1.
- (2) Greenler, R. G. *J. Chem. Phys.* **1966**, *44*, 1, 310.
- (3) Greenler, R. G. *J. Chem. Phys.* **1969**, *50*, 5, 1963.
- (4) Lekner, J. In *Theory of reflection of electromagnetic and particles waves*; Nijhoff Publishers: Dordrecht, The Netherlands, 1987.
- (5) Allara, D. L.; Swalen, J. D. *J. Phys. Chem.* **1982**, *86*, 2700.
- (6) Mielczarski, J. A.; Yoon, R. H. *J. Phys. Chem.* **1989**, *93*, 2034.
- (7) Hoffmann, H.; Mayer, U.; Krischanitz, A. *Langmuir* **1995**, *11*, 1304.
- (8) McIntyre, J. D. E.; Aspnes, D. E. *Surf. Sci.* **1971**, *24*, 417.
- (9) Heavens, O. S. In *Optical Properties of Thin Solid Films*; Dover Publishers: New York, 1965.
- (10) Dignam, M. J. *Appl. Spectrosc. Rev.* **1988**, *24*, 99.
- (11) Bardwell, J. A.; Dignam, M. J. *Anal. Chim. Acta* **1985**, *172*, 101.
- (12) Dignam, M. J.; Mamiche-Afara, S. *Spectrochim. Acta* **1988**, *44A*, 1435.

- (13) Yamamoto, K.; Masui, A.; Ishida, H. *Appl. Opt.* **1994**, *33*, 6285.
- (14) Yamamoto, K.; Ishida, H. *Spectrochim. Acta* **1994**, *50A*, 2079.
- (15) Urban, M. W. In *ATR Spectroscopy: Theory and Practice*; American Chemical Society: Washington, DC, 1994.
- (16) Dong, J.; Ozaki, Y.; Nakashima, K. *J. Polym. Sci., Polym. Phys.* **1997**, *35*, 3, 507.
- (17) Allara, D. L.; Nuzzo, R. G. *Langmuir* **1985**, *1*, 52.
- (18) Porter, M. D.; Bright, T. B.; Allara, D. L.; Kuwana, T. *Anal. Chem.* **1986**, *58*, 2461.
- (19) Boerio, F. J.; Boerio, J. P.; Bozian, R. C. *Appl. Surf. Sci.* **1988**, *31*, 42.
- (20) Kotler, Z.; Nitzan, A. *Surf. Sci.* **1983**, *130*, 124.
- (21) Hansen, W. N. *J. Opt. Soc. Am.* **1968**, *58*, 380.
- (22) Brogly, M.; Nardin, M.; Schultz, J. *J. Appl. Polym. Sci.* **1997**, *64*, 1903.

- (23) Kaito, A.; Nakayama, K. *Macromolecules* **1992**, *25*, 4882.
- (24) Brogly, M.; Bistac, S.; Schultz, J. *Polym. Int.* **1997**, *44*, 11.
- (25) Brogly, M.; Nardin, M.; Schultz, J. *J. Adhesion* **1997**, *58*, 263.
- (26) Jensen, W. B. In *The Lewis acid–base concepts*; J. Wiley & Sons: New York, 1979.
- (27) Fowkes, F. M. *J. Polym. Sci., Polym. Chem. Ed.* **1984**, *22*, 547.
- (28) Brogly, M.; Grohens, Y.; Labbe, C.; Schultz, J. *Int. J. Adhesion Adhesives* **1997**, *17*, 257.
- (29) Hahn, T. D.; Hsu, S. L.; Stidham, H. D. *Macromolecules* **1997**, *30*, 87.

MA971408S